Uncertainties in Hydrologic and Climate Change Impact Analyses in Headwater Basins of British Columbia

KATRINA E. BENNETT

Pacific Climate Impacts Consortium, University of Victoria, Victoria, British Columbia, Canada, and International Arctic Research Center, University of Alaska Fairbanks, Fairbanks, Alaska

ARELIA T. WERNER AND MARKUS SCHNORBUS

Pacific Climate Impacts Consortium, University of Victoria, Victoria, British Columbia, Canada

(Manuscript received 11 August 2011, in final form 8 February 2012)

ABSTRACT

Three headwater basins located across British Columbia (BC) were analyzed using a hydrologic model driven by five global climate models (GCMs) and three scenarios from the Special Report on Emissions Scenarios (SRES) to project future changes in seasonal water budgets and assess the uncertainty in the projections arising from GCMs, emissions scenarios, and hydrologic model parameterizations under two future time periods. Future projected changes in temperature are for annual increases of approximately +2°C by the 2050s and +3°C by the 2080s. The 2050s and 2080s precipitation projections are for increased winter precipitation in all basins and decreases in summertime precipitation for two of the three basins—with increases projected in the northeastern BC subwatershed. The study found that the hydrologic parameter uncertainty ranged up to 55%, (average 31%) for winter runoff anomalies, which was less than the uncertainty associated with GCMs and emissions scenarios that ranged up to 135% and 78% (average 84% and 58%, respectively). The uncertainty results were variable across the three hydroclimate regimes. Coastal headwater systems in British Columbia experience more uncertainty associated with changes during winter and the summer, whereas interior systems experience the greatest uncertainties during the winter and spring. Changes projected for the 2050s at the coastal site fell outside of the range of natural variability, a robust shift that may result in a very different regime for this basin within the short planning horizon of 50 years. A small, semiarid watershed located on the Chilcotin Plateau exhibited changes to the hydrologic regime that were projected to be small in absolute terms and fell within the range of natural variability.

1. Introduction

Preparation for water resource adaptation to climate change requires an understanding of the uncertainty associated with future projections of changes in streamflow and hydrologic budgets. Assessments of future hydrologic impacts that are provided without addressing the associated range of impacts may appear certain but could in fact mislead decision makers who use these results within a management context. Developing a method to assess the uncertainty in hydrologic simulations based on global climate model (GCM) projections will enable managers and decision makers to move forward more effectively with planning and adaptation measures.

Previous work to characterize hydrological responses in the context of the multiple sources of uncertainties present in GCMs, emissions scenarios, downscaling methods, hydrologic models, and the hydrologic model parameter solutions has been considered in a number of research studies (Fowler et al. 2007; Kay et al. 2009; Maurer 2007; Murphy et al. 2007; Nawaz and Adeloye 2006; Prudhomme and Davies 2009a,b; Prudhomme et al. 2003; Tebaldi et al. 2005). Studies have been undertaken on basins worldwide (Todd et al. 2011), in variable hydrologic environments (Horton et al. 2006; Minville et al. 2008), and across different models utilizing contrasting computational methodologies (Bae et al. 2011; Maurer et al. 2010). Other work has examined the uncertainties associated with concurrent future climate change and shifts in land use and soil properties (Feddema

Corresponding author address: Katrina Bennett, International Arctic Research Center, University of Alaska Fairbanks, 930 Koyukuk Drive, P.O. Box 757340, Fairbanks, AK 99775-7340.
E-mail: kebennett@alaska.edu

DOI: 10.1175/JCLI-D-11-00417.1

et al. 2005). Overwhelmingly, these studies show that uncertainty is attributed primarily to the GCMs employed in the study, although many studies allude to the fact that land use is often overlooked and could play a major role in the uncertainty of climate change impacts on hydrology.

In British Columbia (BC), there are few examples of uncertainty analysis for climate impacts studies on hydrology. Examining the impacts of climate change on hydrology and basin water budgets within British Columbia is uniquely difficult owing to ubiquitous nival or mixed-nival watershed regimes across the province, which might be a reason why uncertainty analysis has yet to be undertaken. Modeling in snow-dominated basins, such as those found in the largest of BC's watersheds including the Peace and Fraser River basins, must accurately account for all components of snow accumulation, ablation, and related processes, while also accounting for the correct rainfall patterns present at lower elevations. Measuring hydrologic change in these mountainous watersheds is also difficult because of the lack of representative climate and hydrometric networks that adequately capture the range and variability of historical temperature, precipitation, and streamflow. Conversely, there is a lack of comprehensive, finescale landscape (i.e., vegetation and soils) data available for broad regions to provide consistent parameterizations across the province.

BC has a diversity in hydroclimate regimes that makes it particularly difficult to make assumptions regarding climate impacts owing to the range in orography and synoptic circulation patterns that create complex hydroclimatic interactions across the province (Stahl et al. 2006b). The coarse resolution of GCM grid boxes (~200 to 400 km per side) results in model topographic biases for mountainous regions, which leads to a substantial scalar mismatch between GCM grid and hydrologic model grid boxes, and thus creates an added challenge for downscaling techniques to deal adequately with both climatological biases and topographic relief bias. Thus, there is an outstanding research question regarding the uncertainty associated with the projected impacts from climate change on hydrology of mountainous regions (Bergstrom et al. 2001). For these reasons, presenting uncertainty results based on multiple scenarios and parameters for climate change impact studies in BC watersheds is vital for responsible scientific delivery of climate change impacts on hydrology to water managers and planners working in this region.

This study characterizes uncertainty in hydrologic projections of changes to water balance components because of (i) GCM, (ii) emissions, and (iii) hydrologic parameter uncertainty, which along with downscaling (which is not addressed in this paper) are broadly recognized as the major sources of uncertainty in climate change studies (Arnell 1999). Hydrologic parameter uncertainty is represented by applying 25 different optimal parameter sets or "Pareto solutions" for a hydrologic model. These parameter sets were applied to simulate the hydrologic response using hydrologic model forcings from three different emissions scenarios and five different GCMs, for a total of 15 GCM and emission scenario combinations. Results are presented for temperature and four different hydrologic budget components: precipitation, runoff, snow water equivalent, and evapotranspiration, within the context of "natural variability," which is assessed for the baseline climate. The analysis was run using an implementation of the Variable Infiltration Capacity (VIC) hydrologic model (Liang et al. 1996, 1994), driven by downscaled temperature and precipitation data for the 2050s and the 2080s, in three headwater basins in British Columbia. The basins were carefully selected to represent a range of climatologic, topographical, and hydrological regimes. To the authors' knowledge, this study is the first to assess the uncertainty of climate change projections on hydrology for multiple subwatersheds located across British Columbia using a range of GCMs and emissions scenarios.

The results of this study are anticipated to be useful for water managers, planners, and scientists interested in the uncertainties in climate change and hydrologic impact analyses, especially on the west coast of Pacific North America. The paper is organized as follows: the methodological approach is outlined in section 2 of the paper, followed by a description of the results and discussion of these findings in section 3. Conclusions and future research directions are summarized in Section 4.

2. Methods

a. Model overview and implementation

The VIC hydrologic model is a macroscale model that can be used to simulate the impacts of climate change on large basins (Liang et al. 1996, 1994). The model has been developed in this capacity for several recent studies of climate change impacts in Pacific North America (Christensen and Lettenmaier 2007; Elsner et al. 2010; Hamlet and Lettenmaier 1999; Hamlet et al. 2007). The model was applied at a $1/16°$ grid scale or approximately 28–32 km^2 (dependent on latitude) in BC The model, which explicitly accounts for vegetation effects on snow accumulation, snowmelt, and evapotranspiration, solves the full water and energy balances to generate daily baseflow and quickflow fluxes for individual grid cells.

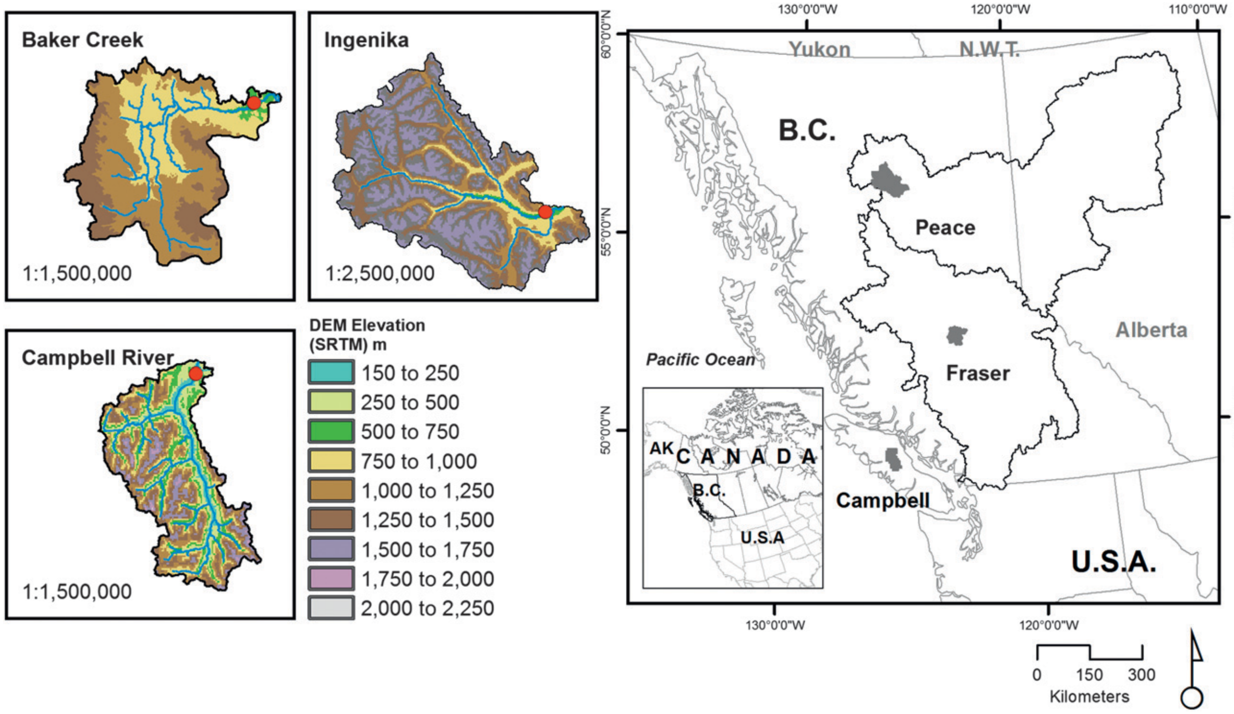

FIG. 1. The three watersheds and subbasins selected for analysis in this study. (right) Subwatersheds situated within their larger basin location in British Columbia with an inset showing the location of British Columbia in North America. (left and middle) The SRTM DEMs for each subbasin. Topographic relief is illustrated using a consistent color ramp to intercompare elevation profiles for each basin. Environment Canada gauges are illustrated with red circles at the outlets of each watershed.

These fluxes are then collected and routed downstream using an offline routing model to simulate streamflow (Lohmann et al. 1998). In this study, the model was driven using boundary conditions of daily maximum and minimum temperature, daily precipitation, and daily average wind speed interpolated from station observations over the period 1950 to 2006. Future daily runoff projections were provided by running the model using daily data that was generated from statistically downscaled monthly GCM projections, as described in section 2d.

Three watersheds across BC were selected for this analysis (Fig. 1). The watersheds range in size from the 4500 km^2 Ingenika River basin to the 1193 km^2 Campbell River basin. Table 1 provides data on basin size and

TABLE 1. Statistics from each basin, including the area of basin (km^2), elevation range, average elevation, hydrologic regime, climate classification, and temperature and precipitation, rainfall, and snowfall statistics. Results are provided for the 1961–90 period.

Basin	Baker Creek	Campbell	Ingenika
Basin characteristics			
Area (km^2)	1564	1193	4500
Elevation range (m)	464–1524	158–2027	672–2303
Average elevation (m)	1089	932	1488
Hydrologic regime	Nival	Hybrid (pluvial–nival)	Nival
Climatic classification	Continental (dry)	Maritime	Continental (humid)
Temperature			
Average minimum January temperature (°C)	−11	−4	−14
Average maximum July temperature (°C)	+15	+16	+13
Precipitation			
Total average annual precipitation (mm)	1161	5716	3000
Total average annual rainfall (mm) and percent (%) of total	648 (56)	4392 (77)	1101 (37)
Total average annual snowfall (mm) and percent (%) of total	513 (44)	1324 (23)	1900 (63)

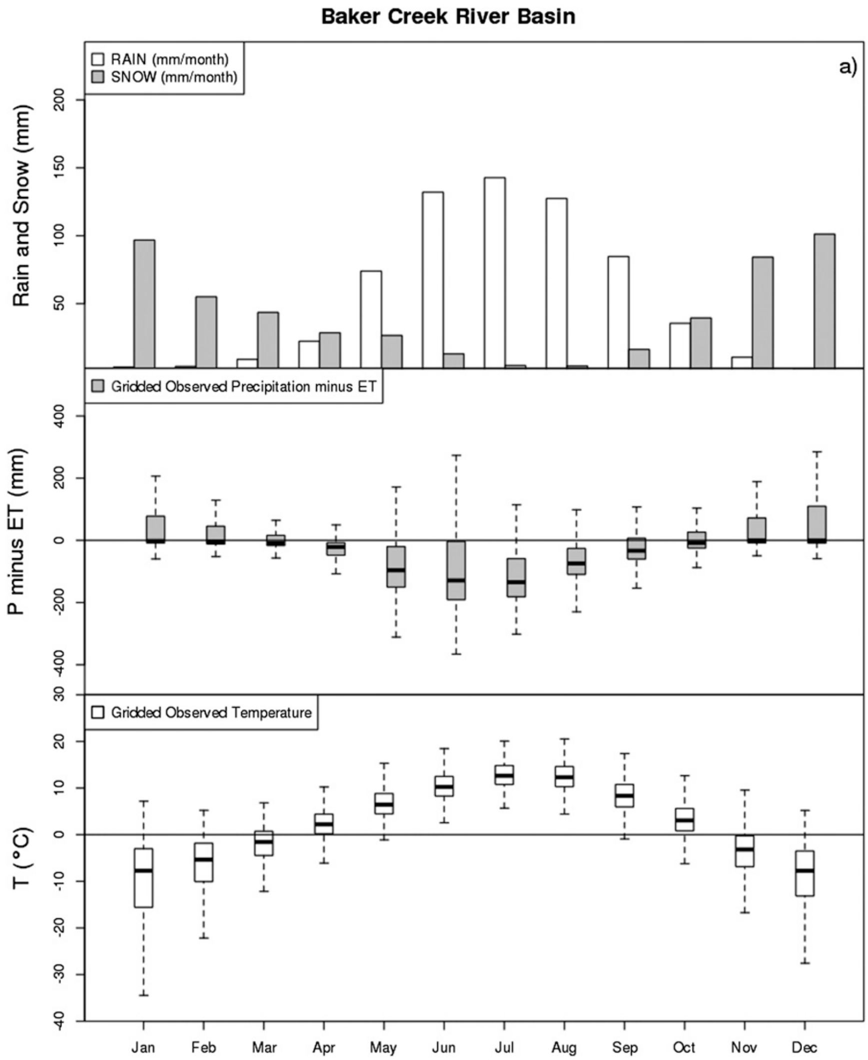

FIG. 2. (top) Simulated (based on observed maximum and minimum temperature and precipitation) rain (RAIN, white bars), and snow (SNOW, gray bars) in mm month^{-1} as barcharts. (middle) Precipitation minus evapotranspiration in mm (*P* minus ET, gray boxes) as box and whisker plots (described in text). (bottom) Mean temperatures in °C (*T*, white boxes): (a) Baker Creek, (b) Campbell, and (c) Ingenika. Data from gridded observed forcing data (described in the text).

other physiographic details, and Fig. 1 illustrates the ranges in topographic relief for each basin. Climate classifications are taken from Demarchi (1996). Baker Creek, situated on the Chilcotin Plateau in the BC interior, is a subwatershed of the Fraser River basin and exhibits bench-like relief across its basin, indicative of its position in the plateau region (Fig. 1). The predominant land cover in Baker Creek is conifer forest. Soils are loam and clay loam at depth (Global Soil Data Task Group 2000). The Campbell River watershed is located on Vancouver Island, and this basin is the most southerly in the study and proximal to the Pacific Ocean (Fig. 1). The Campbell River basin is predominantly covered by conifer vegetation, with alpine tundra at upper elevations (Demarchi 1993). Soils are primarily sandy loams with a thick organic layer overtop (Global Soil Data Task Group 2000). The Ingenika River watershed is located in the Peace River headwaters in the Cassiar Mountain Ranges in north-central BC (Demarchi 1996) and is the largest and most northern of the watersheds examined in this work. It is predominantly forested by conifers, with shrub and tundra at high elevations (MacKinnon et al. 1990). Soils are primarily mineral, with a thin organic layer overtopping the underlying soil horizon. These soils are comprised of rapidly draining morainal and colluvial materials, namely loam, underlain by clay loam at depth

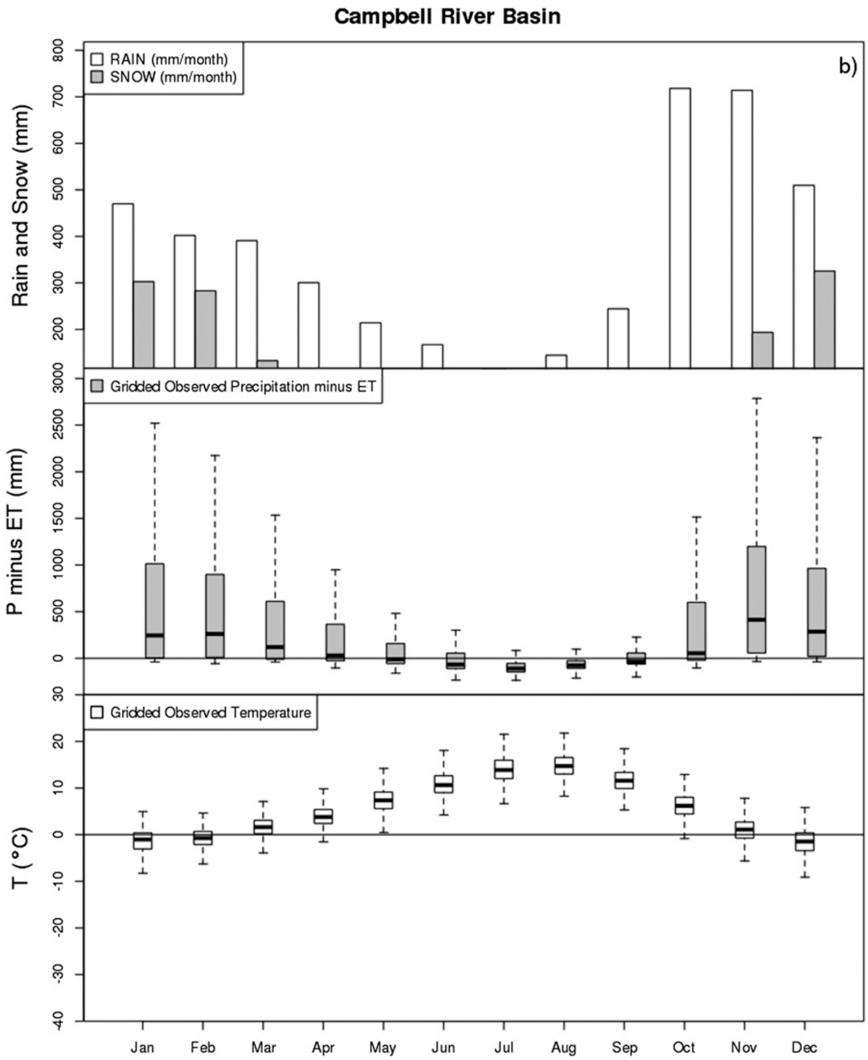

FIG. 2. (*Continued*)

(Centre for Land and Biological Resources Research 1996; Global Soil Data Task Group 2000).

The watersheds share similar characteristics in vegetative cover (primarily conifer forest), soils, and maximum summertime temperatures. The watersheds differ in their size, elevation ranges, and geographic location (Fig. 1) and hence, hydroclimatic regime (Fig. 2, Fig. 3). This is reflected in the different types of precipitation and streamflow regimes observed in each watershed (Table 1, Fig. 3). While the Ingenika and Baker watersheds are interior snow-dominated regimes, the Campbell River stands apart in its hybrid nature. The Campbell River basin receives a higher amount of rainfall than the other basins, with the greatest amount falling during early winter. This is also the most temperate basin of the three, with average wintertime minimum temperatures close to 0°C, but with high elevations contributing snowfall, making it a nival–pluvial regime (Table 1, Fig. 2). The other systems experience comparatively lower amounts of precipitation; the majority of the precipitation peaks in fall and winter, with approximately 50% or greater of winter precipitation falling as snow (Table 1). The Baker Creek watershed is the driest basin of the three examined in this study (Eaton and Moore 2010), its freshet begins in March and peaks in May (Fig. 3). The Ingenika freshet begins in April and peaks in June (Fig. 3). Precipitation exceeds evapotranspiration in the basins for most of the year except in summer; in the Campbell River system this pattern is particularly pronounced during winter in comparison to the other basins. Evapotranspiration (median, black line in box plots in Fig. 2) is greater than precipitation during May to September in the Campbell, while in the interior systems, the median evapotranspiration tends to exceed precipitation

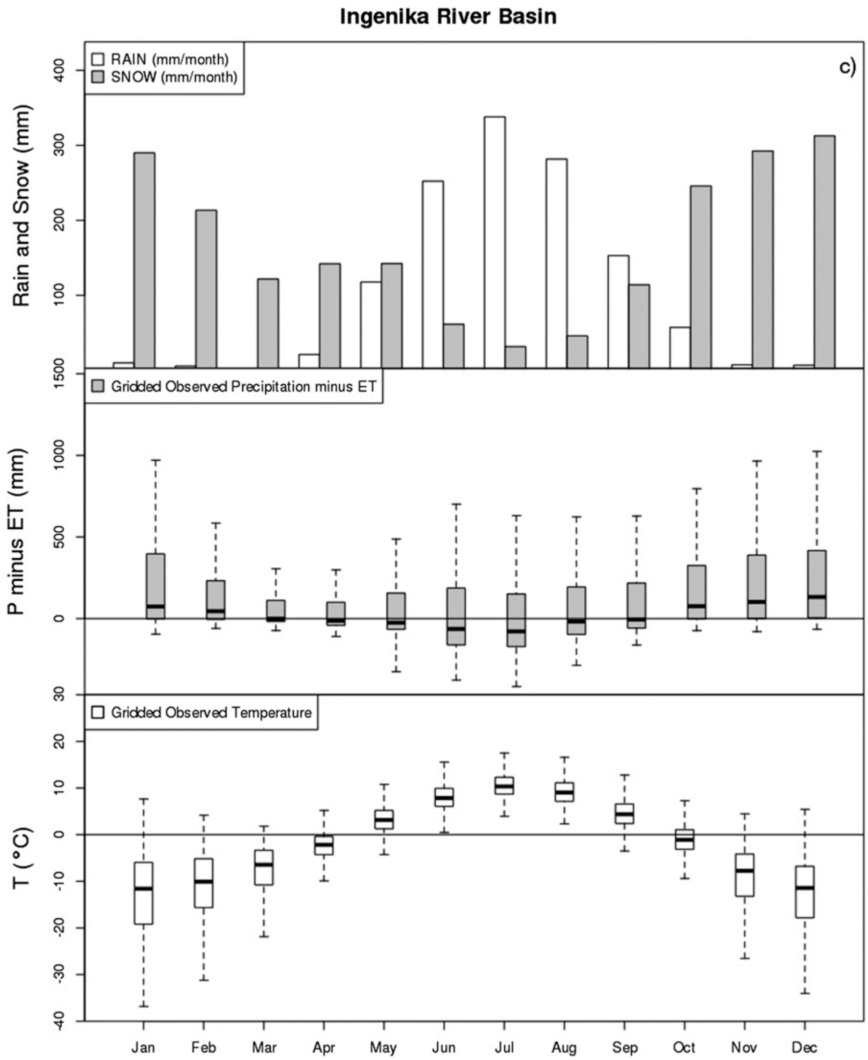

FIG. 2. (*Continued*)

in March through September, elongating the period of moisture deficit.

b. Model parameterization

Gridded climate forcings covering the time period of 1950–2006 at a spatial resolution of 1/16° grid scale were generated based on methods developed by Maurer et al. (2002) and Hamlet and Lettenmaier (2005). Daily National Climatic Data Center (NCDC) Cooperative Observer (COOP) network and Environment Canada (EC) daily station data were interpolated to a 1/16° grid using the Symap algorithm (Shepard 1984). The U.S. Historical Climatology Network (HCN) and Adjusted Historical Canadian Climate Database (AHCCD) data were used to correct for temporal biases caused by inhomogeneities in the COOP and EC station assemblages through time. Daily wind speed surfaces were generated by regridding estimates of 10-m wind speed from the National Centers for Environmental Prediction (NCEP)–National Center for Atmospheric Research (NCAR) reanalysis (Kalnay et al. 1996). A modified version of Precipitation Regression on Independent Slopes (PRISM; Daly et al. 1994, 2002) 1961–90 monthly normals (Hamann and Wang 2005; Wang et al. 2006) was then used to scale precipitation and temperature for orographic influences.

Soil classification was prepared using the Soils Program in the Global Soil dataset (Batjes 1995; FAO 1995; Global Soil Data Task 2000), available at a resolution of 0°5′ (approximately 50 km^2). Some soils parameters were extracted directly from the dataset, and other parameters, such as field capacity, were estimated from empirical formulas (Cosby et al. 1984; Rawls et al. 1993, Fig. 5.1.2 and Table 5.3.3). Soil depths were estimated by

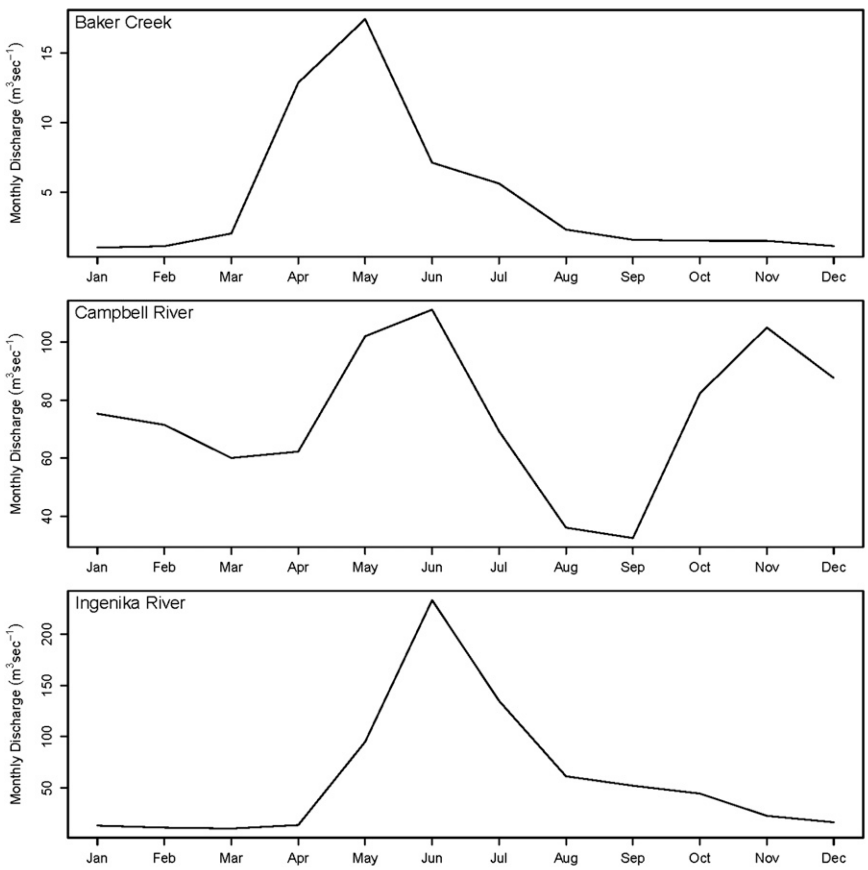

FIG. 3. Monthly average long-term hydrographs using Environment Canada streamflow gauges of the Baker, Campbell, and Ingenika rivers ($m^3\ s^{-1}$). The *y* axis varies based on the maximum flow values (top to bottom) for each watershed. Months are January through to December. Years illustrated are based on data availability: Baker 1974–2003, Campbell 1963–92, and Ingenika 1978–2007.

relating soil depth to elevation and slope using minimum and maximum depth limits of 0.1 and 3.7 m, respectively (the algorithm was originally designed for estimating soil parameters in the University of Washington's DHSVM model). Vegetation parameters were developed using the 1-km modally indexed Earth Observation for Sustainable Development (EOSD, circa 2000) land cover classification (Wulder et al. 2002). Monthly leaf area index (LAI), a key variable required to calculate water budgets in forested regions, was measured for each land cover class based on the Canada-wide 1-km monthly SPOT4-Vegetation LAI 10-day time series (Latifovic 2006). Subgrid topography is represented in the VIC model via the application of elevation bands; a maximum of five elevation bands per grid cell is used in this model implementation. The Consultative Group on International Agricultural Research (CGIAR)–Consortium for Spatial Information (CSI) Shuttle Radar Topography Mission (SRTM) digital elevation model (Jarvis et al. 2008) was used to develop elevation bands.

c. *Model calibration and validation*

The VIC model simulates fluxes, such as runoff, baseflow, evapotranspiration, and snowmelt, for each grid cell but applies a separate routing model to transport surface runoff and baseflow from each grid cell through the river system (Lohmann et al. 1998). Modeled and observed daily streamflow are compared during calibration, using a continuous observed streamflow record from Environment Canada. Calibration in the VIC hydrologic model is achieved primarily by adjusting the soils parameters that were not explicitly defined by the soils classification, namely infiltration and baseflow parameters that moderate the rate and volume of water that enters and exits the soil column. The method results in uniform values for each calibration parameter across grid cells within each calibrated basin. The basins are validated using an alternate time period to the calibration period (referred to as a split-sample approach to model calibration and validation, see Singh and Woolhiser 2002).

TABLE 2. Hydrologic parameter ranges applied for calibration in this study.

Parameter	Range
BI	0.00001–0.5
Ds	0.00001–0.05
Ws	0.05–1.0
EXPN	1.0–3.0
Dsmax	0.1–30.0
PADJ	0.7–1.3

For this application six parameters governing infiltration, percolation, baseflow, and precipitation amount are used for calibration. The B-infiltration (BI) parameter describes the amount of available infiltration capacity as a function of relative saturated grid cell area. Three parameters define baseflow, namely Dsmax, the maximum baseflow that can occur in one day in mm day^{-1}, Ds, the fraction of Dsmax where nonlinear baseflow begins, and Ws, the fraction of maximum soil moisture where nonlinear baseflow occurs. The exponent parameter from the Brooks–Corey relationship EXPN, (e.g., Table 5.1.1 in Rawls et al. 1993) was also included in the model calibration. This parameter empirically defines the pore size distribution of soils and constrains the ability of the soils to retain water; a large value of this number indicates uniform pore sizes and leads to a greater water retention, that is, lower runoff and baseflow and higher evapotranspiration. The parameter ranges are defined based on values determined from previous VIC applications (Table 2, Fig. 4; Schnorbus et al. 2010; Shi et al. 2008).

Within the complex topography of BC where precipitation is spatially variable, bias in precipitation data is unavoidable. Bias is a result of a climate network with low station density weighted toward lower elevations (Adam et al. 2006; Stahl et al. 2006a) and subject to gauge undercatch, particularly for solid precipitation (Adam and Lettenmaier 2003). Consequently, these precipitation bias correction factors are commonly required for modeling alpine hydrology and are a feature of hydrology models applied in BC (e.g., Quick 1995; Stahl et al. 2006a). Thus, an adjustment is applied in this study to correct for precipitation bias PADJ. This adjustment varies by basin and is diagnosed during the automatic calibration process [Multi Objective Complex Evolution (MOCOM), described below] to correct for over or underestimation of the observed mean annual volume of runoff. Streamflow errors diagnosed from long-term water balance modeling suggest that precipitation bias throughout BC is most frequently between +30% and −30% (Moore et al. 2011).

Calibration of the six selected parameters was performed using the automated MOCOM method (Yapo et al. 1998). MOCOM is a technique that treats hydrologic

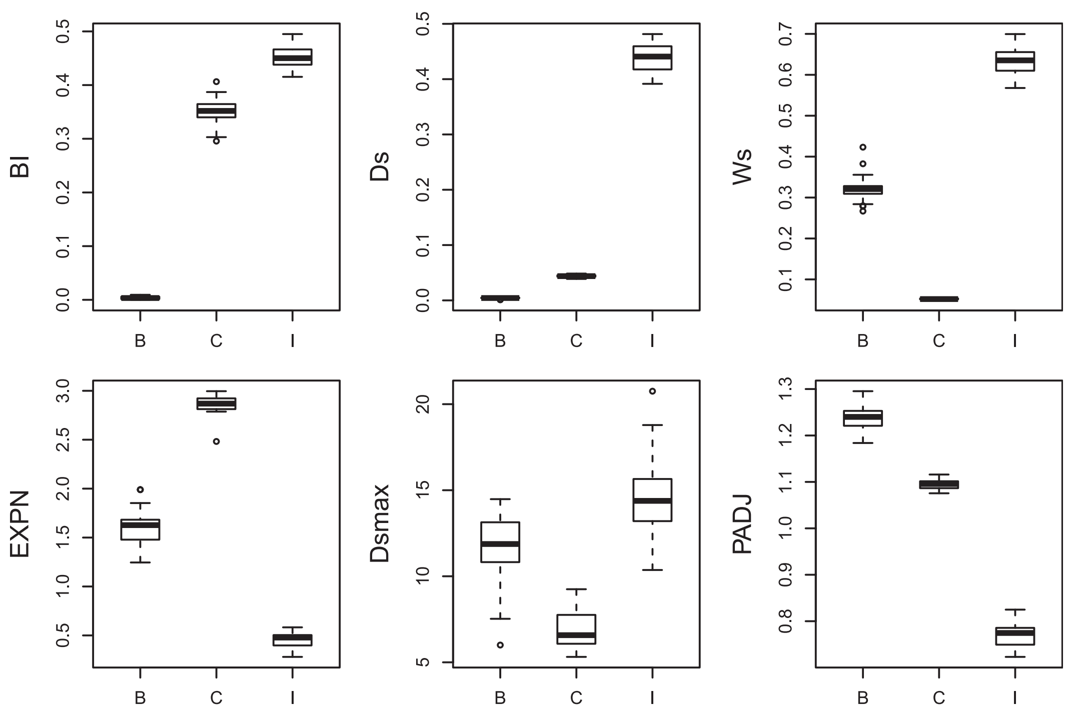

FIG. 4. Resulting range in Pareto sets for each hydrologic parameter calibrated for each watershed (B = Baker, C = Campbell, I = Ingenika).

model calibration as a multiple objective global optimization problem without a unique solution. Therefore, MOCOM provides the so-called Pareto set solution, which is the set of all parameter vectors that produce nondominated values of the objective functions. For the current application a Pareto set of 25 parameter vectors was generated for each study basin (Fig. 4 illustrates the results of these for each calibrated parameter and all watersheds). Three performance measures (objective functions) were applied in this analysis: Nash–Sutcliffe (NS; Nash and Sutcliffe 1970) of daily discharge, Nash–Sutcliffe of the daily log-transformed discharge (NSlog), and the relative volume bias (VB). The NS function predominantly responds to the magnitude of phase and timing errors in daily discharge but is also affected to a lesser degree by the presence of bias between the observed and modeled runoff. The NS function emphasizes the high–peak flow periods and therefore produces parameters that optimize hydrograph performance during the freshet. The NSlog objective tends to place more uniform emphasis through the entire flow range and therefore will generate parameter sets that have better hydrograph performance during the recession and low flow periods of the annual hydrograph. The VB objective strictly emphasizes volume conservation over the calibration period and is not responsive to errors in streamflow timing or seasonality.

The calibration approach assumes that the calibrated parameters are stationary in that they are valid under both the historical and projected climate (Prudhomme and Davies 2009a). This is considered a reasonable assumption because the transformation of rainfall and snowmelt to streamflow is representative of underlying physical processes (i.e., soil properties and infiltration, and baseflow constraints based on the translation of water through the soil column) that are assumed to remain consistent over the next 100 years. Further, many of the processes in the VIC model, which are uncalibrated (such as evaporation, transpiration, and snowmelt) are physically based, allowing for more confident extrapolation of hydrologic processes into unobserved future climate regimes (Leavesley 1994; Ludwig et al. 2009). Nevertheless, the assumption of stationarity is likely not held with regards to land cover; however, the explicit incorporation of dynamic land cover is outside the scope of the current study.

d. *Future GCM emissions scenarios selection and downscaling technique*

The Coupled Model Intercomparison Project phase 3 (CMIP3) archived 25 models as part of the Lawrence Livermore National Laboratory's (LLNL's) Program for Climate Model Diagnosis and Intercomparison (PCMDI; Meehl et al. 2007). Because of the extensive modeling and processing required to analyze the influence of each GCM and emissions scenarios on projected hydrologic and water balance changes on three watersheds in BC, a subset of all available GCMs was applied in this work. The methodological approach to select the GCMs was aimed at maintaining a range in future projected climate changes and evaluating model performance based on past records. This approach does not provide information on future model performance but provides support for their credibility and is one of the only means available to evaluate GCMs (Knutti 2008; Knutti et al. 2010b). Given these constraints, a solid rationale is outlined for model selection based primarily on recent studies documenting GCM performance.

Gleckler et al. (2008) was used to screen model performance over the globe and the Northern Hemisphere. Models were eliminated if their relative error was greater than 50% of the "typical" model error when compared to observational datasets for multiple climatic variables globally. Additionally, selected models were ranked within the top 10 according to the Model Climate Performance Index (MCPI) in the Northern Hemisphere, which combines comparisons of multiple variables as simulated by GCMs to observed values (Gleckler et al. 2008). Models were also screened based on their performance for several metrics over North America and western North America. Radic and Clarke (2011) evaluated the CMIP3 models that had sufficient available data over both of these domains using much of the same metrics applied by Gleckler et al. (2008) including the MCPI. Additionally, they evaluated the model skill in replicating variability in the climate system created by modes such as the El Niño–Southern Oscillation (ENSO) and the Pacific decadal oscillation (PDO) using the model variability index and tested the ability of models to mimic the characteristic synoptic patterns found in the North American Regional Reanalysis for each season using self-organizing maps (Radic and Clarke 2011). Those models not ranked as lowest in any category were considered for selection. Based on all of these metrics, five of the most robust GCMs (identified in Table 3) were selected for this work.

Run one from the CMIP3 monthly ensemble database is most widely available and hence was applied in this analysis. Three Special Report on Emissions Scenarios (SRES) (Nakicenovic et al. 2000) emissions scenarios, covering a range of low, medium, and high projected emissions scenarios (B1, A1B, and A2, respectively) to the end of the twenty-first century were included to test the influence of emissions scenario uncertainty. The ALL forcings (GHG, aerosols, solar, volcanic) scenario was used as the historical baseline in all selected models.

TABLE 3. Modeling laboratory, GCM, version, and abbreviation, followed by codes used for GCM and emissions scenarios versions used in the study and referred to in text and figures. The numeric order for the x axis in Fig. 7 is also provided.

Modeling laboratory (GCM name and version)	Naming code (used in text)	Emissions scenarios	Numbering in Fig. 6
Geophysical Fluid Dynamics Laboratory Climate Model version 2.1	GFDL2.1	B1, A1B, A2	1, 6, 11
Hadley/Met Office third climate configuration of the Met Office Unified Model (HadCM3)	HadCM3	B1, A1B, A2	2, 7, 12
Max Planck Institute for Meteorology ECHAM5	ECHAM5	B1, A1B, A2	3, 8, 13
Community Climate System Model, version 3	CCSM3	B1, A1B, A2	4, 9, 14
Canadian Centre for Climate Modelling and Analysis Coupled General Circulation Model, version 3.1 (T47)	CGCM3	B1, A1B, A2	5, 10, 15

The spread of the readily accessible CMIP3 models (22 of the 25 from PCMDI) is shown for the 2050s winter and summer in Figs. 5a, and 5b, respectively. All available run 1 models were compared to the 15 GCMs and emissions scenarios selected for this work. In the wintertime [December–February (DJF), Fig. 5a], the model spread captured by the 15 GCM and emissions scenarios used in this study extends over the range of the available CMIP3 models with the exception of the most extreme warm/dry and warm/wet conditions exhibited by a few model scenarios combinations. For the Ingenika, Campbell, and Baker basins, run 1 of the Institute of Atmospheric Physics (IAP) Flexible Global Ocean–Atmosphere–Land System Model gridpoint version 1.0 (FGOALS-g1.0) GCM run under the A1B emissions scenario provides this extreme condition. The FGOALS-g1.0 GCM appears to have known biases (i.e., Randall et al. 2007) and was ranked in the lower categories (ranked 21st or 22nd out of 22 models) for two performance metrics over North America (see Fig. 7 in Radic and Clarke 2011). In the summer [June–August (JJA), Fig. 5b], the selected model spread represents the range of conditions with the exception of the extreme warm–dry conditions. The U.K. Hadley Centre Global Environmental Model (HadGEM) model run under the A1B emissions scenario for the Baker and Campbell provides the extreme warm and dry projection. The U.K. HadGEM model was excluded from this study because it does not have a B1 run and therefore would not retain the balance in the tri-emission scenario approach used for this work. Additionally, the U.K. HadGEM did not have sufficient data available for it to be fully evaluated under the Radic and Clarke (2011) study.

GCM emissions scenarios were downscaled using a technique referred to as Bias Correction Spatial Disaggregation (BCSD, based on methods described by Salathe 2005; Widmann et al. 2003; Wood et al. 2002). BCSD is a widely applied statistical downscaling technique, which has been shown to be one of the more successful approaches for downscaling the coarse-resolution GCM results (Hayhoe 2010). BCSD's strengths include the ability to capture projected changes across all percentiles, an approach to local scaling that accounts for local and regional spatial variability, and applicability in creating gridded data suitable for driving spatially distributed hydrologic models (Salathe et al. 2007; Werner 2011; Wood et al. 2004). BCSD is calibrated for each individual GCM against the gridded historical forcing dataset (described in section 2b) based on the 1950–99 period. The quantile mapping bias correction ensures that the monthly mean and variances of the gridded observed data are matched in the corrected GCMs (Wood et al. 2004). The GCM versus BCSD winter temperature and precipitation anomalies are illustrated in Figs. 6a and 6b, respectively.

The statistical paradigm that informs our methodology of GCM selection and interpretation of climate projections can be classified as ''indistinguishable weighted'' (Knutti et al. 2010a). The use of five of the original suite of models from CMIP3 effectively applies a binary weighting (i.e., 0 or 1) to the full set of results. Climate projections from the final ensemble of GCM runs are treated as statistically indistinguishable (Annan and Hargreaves 2010; Knutti et al. 2010a). Each ensemble member is considered indistinguishable from all possible outcomes of the earth's chaotic processes (Annan and Hargreaves 2010). Also, each of the emissions scenarios is treated as an equally likely assumption of the possible trajectory of atmospheric greenhouse gases over the coming century (Bray and von Storch 2009).

e. Uncertainty analysis

The hydrologic model was run from 1950 to 2099 using the set of 25 Pareto solutions (unique parameterizations) for each of the five GCMs and three emission scenario combinations for a total of 375 simulations in each subbasin. The range in uncertainty resulting from BCSD downscaled GCMs, emissions scenarios, and parameter sets for each basin are presented as boxplots of the projected anomalies for several water balance variables: runoff, snow water equivalent, and

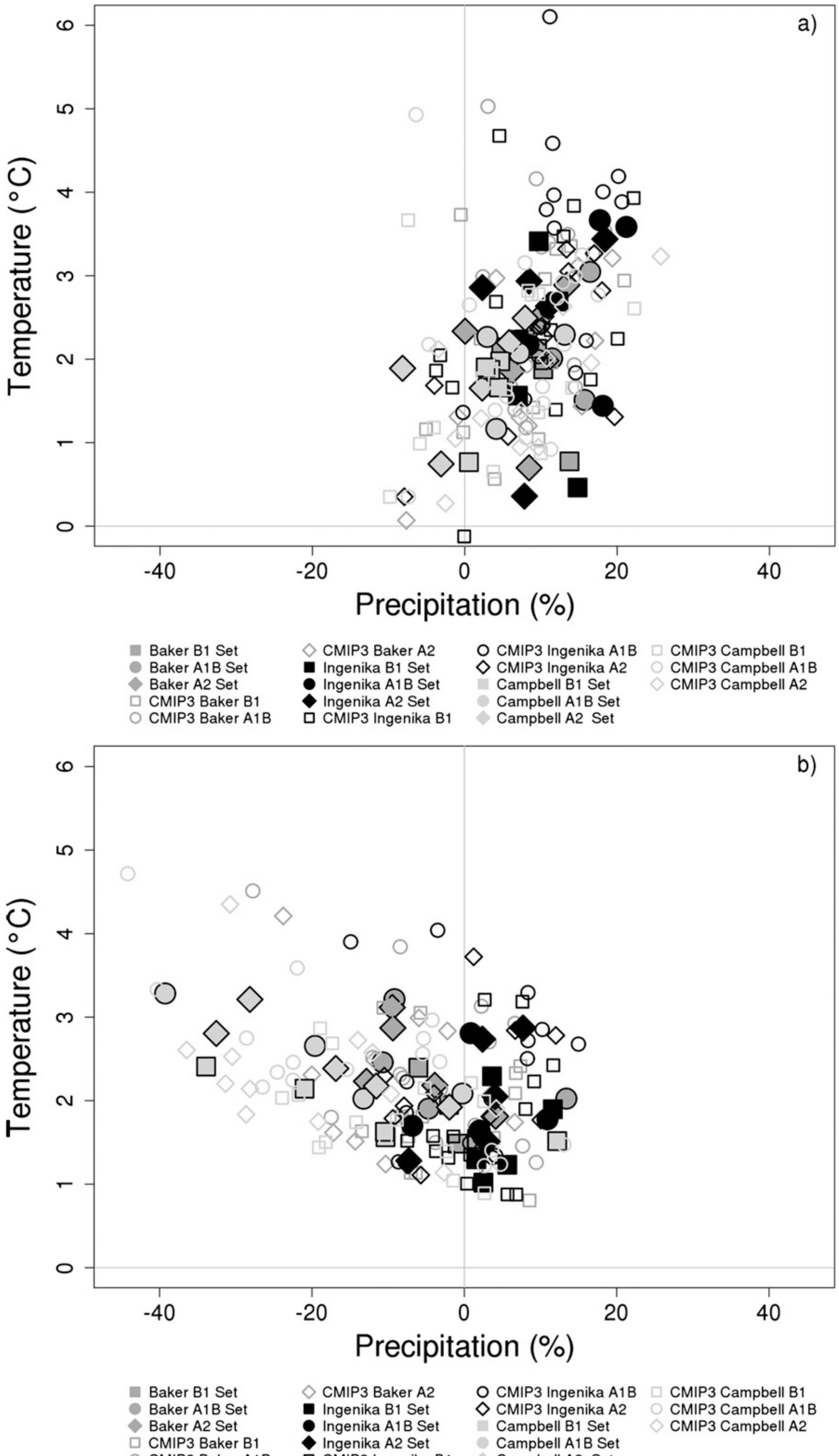

FIG. 5. The range of models from the CMIP3 GCMs (22 of the 25 models) plotted (open symbols) against the 15 GCMs and SRES emissions scenarios (filled symbols) selected for this study for (a) winter and (b) summer for the 2050s in the basins analyzed (see legend).

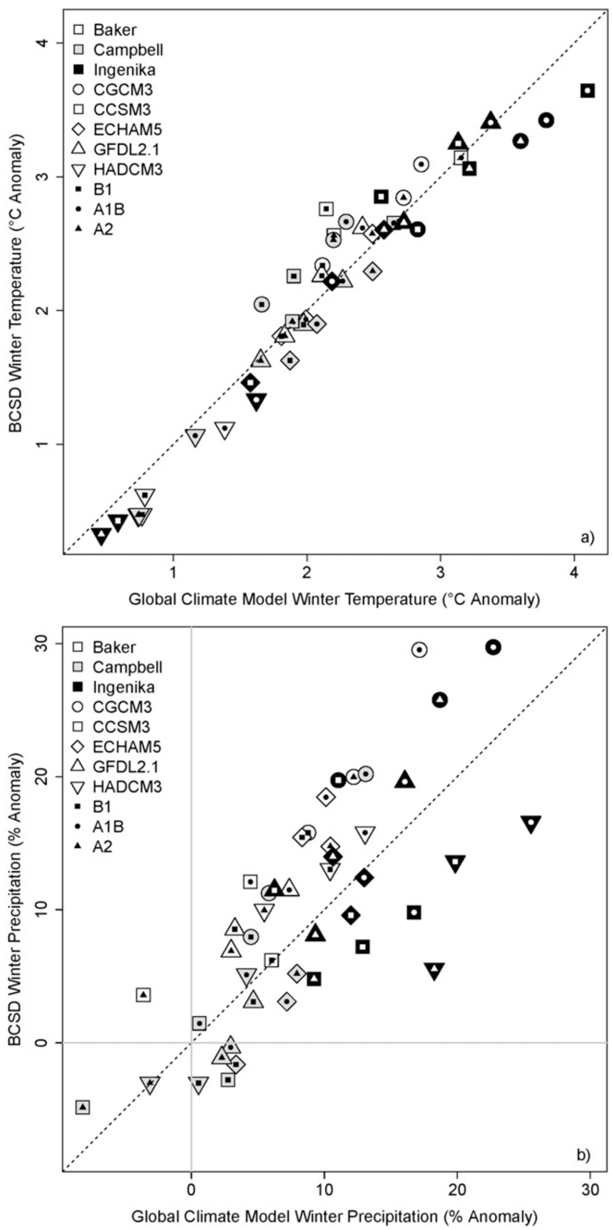

FIG. 6. Scatterplots illustrate the relationship of the GCM input data compared to downscaled BCSD results for anomalies of (a) winter temperature (°C) and (b) winter precipitation (%). Results for Baker Creek are illustrated in clear, Campbell River in gray, and Ingenika in black symbols. Each global climate model and impacts scenario is illustrated with corresponding symbols as shown in the legend.

evapotranspiration. Percentage anomalies are calculated by subtracting the future GCM and emissions scenarios by the median of all of the historical GCM scenarios (1961–90 baseline), dividing by the median baseline, and multiplying by 100. The boxplots illustrate, for each GCM and emissions scenarios anomaly, the first and third quartile ranges (box), the median (dark line), 1.5 times the interquartile range (whiskers), and outliers (circles) of the projected changes from all 25 Pareto solutions. The analysis was undertaken for two future time periods (the 2050s as 2040–69, and the 2080s as 2070–99). The future time periods begin on the even climatological year, for example, 2040 and not 2041) because not all GCM model runs were available for the last year of the twenty-first century. Nevertheless, we chose to retain the commonly accepted definition of 1961–90 for the historical period.

To place the future changes in context of the historical range or natural variability of a given variable, the coefficient of variation is included as a backdrop to the boxplots. The coefficient of variation is a normalized measure of dispersion used to quantify historical interannual variability, which incorporates elements of both low-frequency (e.g., PDO) and high-frequency variability (e.g., ENSO). The coefficient of variation was estimated from the seasonal mean and the standard deviation over the historical period (1961–90) for all water balance variables as

$$\mathrm{Cv}_s = 100(\sigma_s/\mu_s),$$

where μ_s and σ_s are the estimated seasonal mean and sample standard deviation, respectively. The Cv_s is given as a relative anomaly to the 1961–90 period for each GCM emission scenario, averaged across hydrologic parameterizations.

The differences between hydrologic projections resulting from the use of different downscaled GCM emissions scenarios are referred to as GCM and emissions uncertainty, while the differences between hydrologic projections based on the use of separate parameter solutions sets is referred to as hydrologic parameter uncertainty. GCM uncertainty is tested by comparing the range between GCMs run under the same emissions scenario, while emissions uncertainty is tested by comparing the range over all three emissions scenarios, that is, A1B, A2, or B1 for one GCM. Statistical significance was included using a Wilcox test for two samples to determine if future changes were statistically different at the 5% significance level; significantly different samples are illustrated in Figs. 7a–l by gray triangles.

3. Results and discussion

a. *Model calibration and validation results*

Because of the limitations in the forcing data and ranges in hydroclimatic complexity, not all basins calibrate equally well under the same approach. This divergence amongst basins may have implications for the range in parameter uncertainty and therefore is discussed

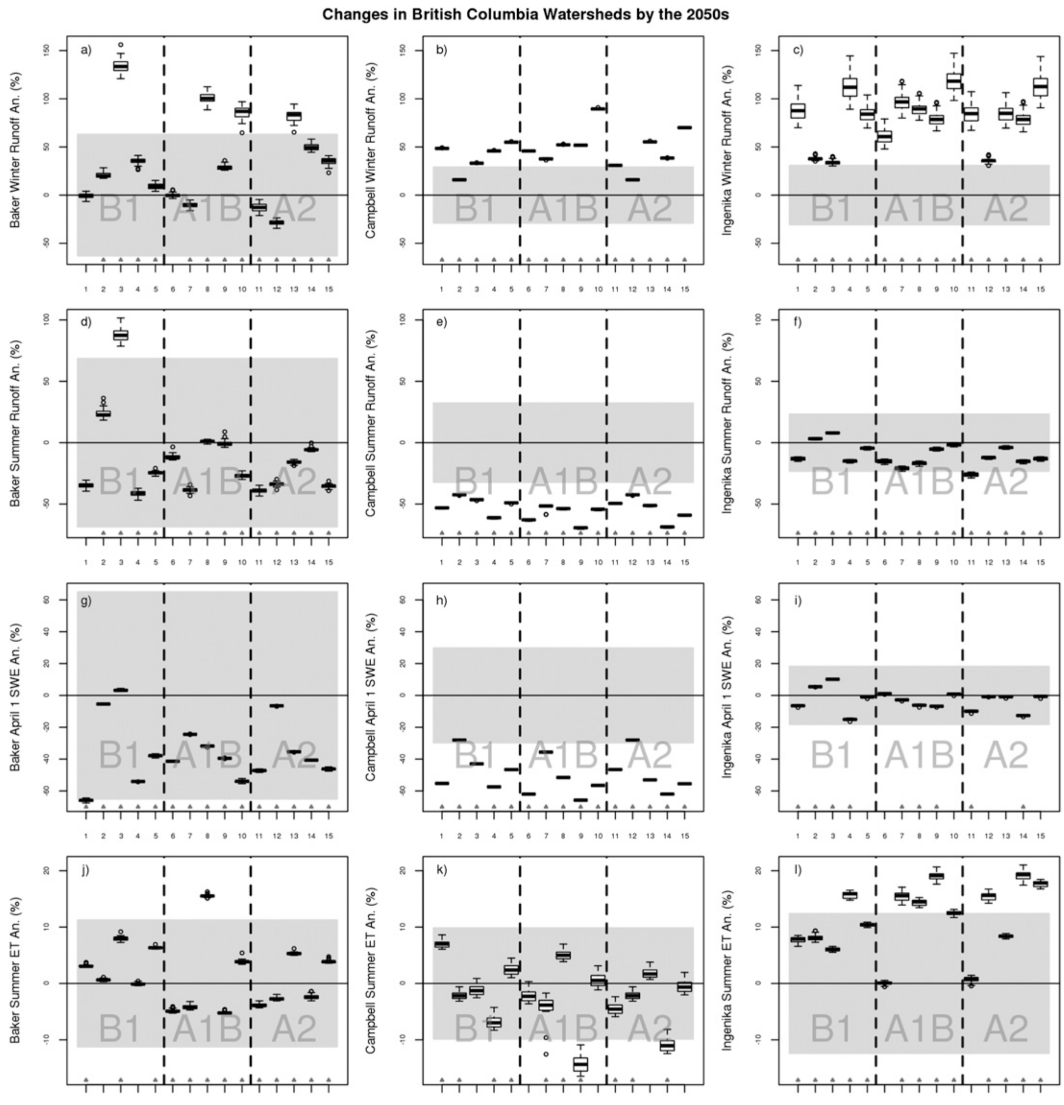

FIG. 7. (top to bottom) Projected range in winter (DJF), summer (JJA) runoff, 1 Apr SWE, and summer (JJA) ET anomalies (%) for (left to right) the Baker, Campbell, and Ingenika River basins to the 2050s for GCM emissions scenarios (each box and whisker) compared to Pareto set results (range of box and whiskers plots). Boxplots are described in the text. Corresponding numbers are provided in Table 5. The coefficient of variation as a percentage is calculated using the historic record (1950–2006), shown by gray boxes. Statistically significant (5% significance level) scenarios are illustrated with small gray triangles. Table 3 lists numerical order for the GCMs on the *x* axis.

further here. Model calibration and validation results are summarized in Table 4 for the 25 hydrologic parameterizations for each basin. For the calibration period, NS mean values range from 0.63 (Baker) to 0.72 (Campbell). NSlog results tend to be higher for most watersheds, indicating that during the calibration period, the calibration approach was better able to tune the model to simulate baseflow more so than runoff peaks (Table 4). The exception is the Campbell River basin, where the NSlog is lower than the NS value. This result may be expected in the Campbell River basin because of its mixed rainfall–snowmelt streamflow regime. Because of the (limited) calibration parameters in the VIC model and the simplicity of the routing model, it was challenging to calibrate both the peaks and recessions of rainfall and snowmelt events equally. NSlog and NS statistics ranged the most in hydrologic parameterizations in the Ingenika basin (standard deviations of 0.04 and 0.05 for NS and NSlog, respectively). Volume bias ranged the most in the Baker Creek watershed during the calibration and validation period as indicated by a standard deviation of 5%, and the least in the Campbell

TABLE 4. Summary of calibration and validation results (maximum, mean, minimum, and standard deviation) from the 25 Pareto parameter solution sets for three performance measures, for each river basin. The calibration and validation time period is provided. The quantity NS is Nash–Sutcliff, NSlog is log Nash–Sutcliff, and VB is the percent volume bias of runoff.

Basin		Baker			Campbell			Ingenika		
Calibration period		1985–90			1990–95			1990–95		
		NS	NSlog	VB	NS	NSlog	VB	NS	NSlog	VB
Calibration	Max	0.65	0.80	25	0.73	0.59	4	0.78	0.84	17
	Mean	0.63	0.79	17	0.72	0.57	2	0.68	0.78	10
	Min	0.59	0.77	6	0.70	0.52	0	0.62	0.65	4
	SD	0.01	0.01	5	0.00	0.02	1	0.04	0.05	4
Validation period		1991–95			1985–89			1985–89		
Validation	Max	0.61	0.76	35	0.73	0.68	8	0.86	0.84	16
	Mean	0.57	0.72	28	0.72	0.66	6	0.83	0.75	5
	Min	0.48	0.64	18	0.71	0.62	4	0.81	0.58	0
	SD	0.03	0.03	5	0.00	0.02	1	0.01	0.07	4

(1%). The larger ranges in statistics suggest more sensitivity to the calibrated parameters BI, Ds, Dsmax, Ws, EXPN, and PADJ in the Baker and Ingenika basins. Volume bias tends to be lower during the calibration period in Baker and Campbell and higher in Ingenika compared to the validation period, which might be due to some overfitting from the use of the PADJ calibration parameter in the Baker and Campbell River basins.

Generally, in the validation period, mean NS statistics were reduced, although this was not the case for the Ingenika River basin, where results improved from the calibration period. In 1990, there was one very large peak flow event recorded for Ingenika that was not captured by the model (not shown). During the validation period, 1985–89, there were no such anomalous events, thus NS values were higher.

b. *Impact of downscaling on GCM emissions scenarios by basin*

GCM projections were downscaled to a $1/16°$ grid-scale resolution to make them suitable for driving the hydrologic model. Here we explore the influence of BCSD downscaling on the projected temperature and precipitation change. As only one downscaling approach is being used we intend to show how it modifies the GCM signal before discussing the range of uncertainty introduced by the GCMs and emissions scenarios.

Downscaled projected temperature and precipitation changes for each of the 15 scenarios were analyzed for the 2050s for all basins and seasons (Figs. 6a and 6b, spring, summer, and fall, not shown). In the winter, by the 2050s, projected temperature changes fall close to the 1:1 line for all GCM emissions scenarios combinations (Fig. 6a). In summer (not shown), projected temperature increases were amplified by the BCSD process by nearly one degree under all GCMs, emissions scenarios, and in most basins, while some were reduced by up to one degree (HadCM3; Campbell). Precipitation anomalies in winter in the 2050s were amplified in the Baker Creek basin and reduced in the Campbell and Ingenika basins, under most scenarios by $\sim\pm15\%$ (Fig. 6b). This reflects the local scaling inherent in the BCSD process, which corrects precipitation signals from the GCM to better match regional variability in precipitation due to orography and distance from the ocean. Summer precipitation anomalies (not shown) were modified less so by BCSD, to within $\sim\pm10\%$ for most models and basins. The HadCM3 A1B projection in the Campbell basin was the only model that was adjusted by approximately 20% (from $\sim-40\%$ to $\sim-20\%$). Thus, while the downscaling technique bias corrects the GCM results against gridded observations to provide precipitation and temperature projections at a spatial and temporal scale appropriate for use with the VIC model, the technique does not vastly alter the projected anomaly on a seasonal basis. BCSD maintains the monthly patterns of the GCM and corrects proportionally by quantile for each grid tile (Wood et al. 2004), therefore it likely modifies the projected transient change from the GCM less than more coarse techniques, such as the delta approach, which provide bias corrections based on a 30-yr average, uniformly across basins and distributions (Elsner et al. 2010).

c. *Uncertainty analysis*

Uncertainty in projected runoff anomalies were analyzed for all seasons and annually for two future time slices and are summarized in Table 5. Projected differences are shown as percentage anomalies from the median historical GCM emission scenario, organized by season. This normalizes the results across the three basins. Results illustrate a range in variability across all watersheds against the historical median scenario. During the season with the largest relative change (winter, December–February), the range within the boxplots (hydrological parameter distribution, maximum anomaly range 55%) is less than the range between GCM scenarios (maximum anomaly range 135%; Table 5; Fig. 7a) and the emissions scenarios (maximum anomaly range of 78%, Table 5; Fig. 7a). Spring runoff changes (not shown) are similar to the changes observed in winter but are of slightly smaller magnitude for the snowmelt dominated systems. In the Campbell, changes are of a much smaller magnitude in spring. Winter runoff increases for most watersheds and scenarios and decreases in summer (Figs. 7a–c and 7d–f, respectively).

TABLE 5. 2050s and 2080s runoff ranges for the % anomaly for winter (December–February), spring (March–May), summer (June–August), and fall (September–November), and annually for the hydrological parameter sets. The minimum represents the range between min and max percentage anomalies for all 25 parameter sets for one projection—GCM and emissions scenario (i.e., CGCM3 A2), and maximum represents the range between min and max percentage anomalies for all 25 parameter sets for one projection—GCM and emissions scenario (i.e., GFDL2.1 B1). The count of the number of GCMs and emissions scenarios that fall outside natural variability is also provided (NV), except for annual averages. For emissions scenarios and GCMs, the difference in median percent anomalies for the 5 GCMs run under B1, A1B, and A2 is provided. Maximum difference in median percent anomalies due to the B1, A1B, and A2 emissions scenarios by GCM (i.e., CCSM3) (B = Baker, C = Campbell, I = Ingenika).

		Winter				Spring				Summer				Fall				Annual			
2050s runoff for each basin	Range	B	C	I	Avg	B	C	I	Avg	B	C	I	Avg	B	C	I	Avg	B	C	I	Avg
Range due to hydrologic parameterizations per projection	Min	9	1	8	6	6	0	1	2	4	1	2	2	3	0	3	2	3	0	0	1
	Max	35	2	55	31	24	2	13	13	23	7	5	12	48	16	12	25	16	2	1	6
	NV	4	13	15	11	4	0	14	6	1	15	1	6	1	1	3	2	—	—	—	—
Range between GCMs run under B1 emissions scenarios	Total	135	39	78	84	115	17	58	63	129	19	23	57	117	21	24	54	115	12	8	45
Range between GCMs run under A1B emissions scenarios	Total	111	52	58	74	63	9	46	39	40	18	19	26	51	37	36	41	61	23	13	32
Range between GCMs run under A2 emissions scenarios	Total	111	54	77	81	63	11	49	41	33	26	22	27	58	28	20	35	56	17	10	28
Range between emissions scenarios by GCM	Max	78	35	61	58	9	54	103	55	24	77	27	43	71	12	9	31	71	12	9	31
Range due to GCMs, emissions scenarios and hydrologic parameterizations	Total	162	74	84	107	125	17	81	74	129	27	34	63	119	40	36	65	128	25	17	57
		Winter				Spring				Summer				Fall				Annual			
2080s runoff for each basin	Range	B	C	I	Avg	B	C	I	Avg	B	C	I	Avg	B	C	I	Avg	B	C	I	Avg
Range due to hydrologic parameterizations per projection	Min	8	1	27	12	6	1	5	4	3	2	3	3	5	0	9	5	3	0	0	1
	Max	45	4	107	52	21	3	36	20	14	7	6	9	47	17	18	27	14	2	1	6
	NV	6	15	15	12	5	2	15	7	0	15	8	8	1	2	9	4	—	—	—	—
Range between GCMs run under B1 emissions scenarios	Total	118	33	67	73	92	12	44	49	57	16	12	28	102	30	17	50	88	16	10	38
Range between GCMs run under A1B emissions scenarios	Total	192	51	141	128	54	12	56	41	45	6	16	22	61	31	43	45	65	14	9	29
Range between GCMs run under A2 emissions scenarios	Total	258	70	130	153	85	34	85	68	32	18	20	23	57	53	50	53	93	26	13	44
Range between emissions scenarios by GCM	Max	115	42	155	104	51	22	72	48	49	22	22	31	61	15	23	33	51	12	9	24
Range due to GCMs, emissions scenarios and hydrologic parameterizations	Total	258	85	183	175	116	34	116	89	64	29	35	43	118	53	50	74	107	26	15	49

As stated above, the greatest amount of spread is observed between projections from multiple GCMs across all watersheds. The GCM anomaly range in winter runoff for the 2050s (Fig. 7a; Table 5) is greatest in the Baker Creek watershed (135% for the B1 scenarios); runoff projections in this watershed may be positive or negative depending on the GCM under consideration. The large percentage anomalies for Baker Creek under the B1 scenario in winter (Fig. 7a) and summer (Fig. 7d) are due in part to low absolute runoff during these periods in the historical record. This is likely due to the lack of a marked increase in temperatures under these scenarios by the 2050s (and hence preservation of snow cover; see Fig. 7b) and projected higher fall (not shown) and wintertime precipitation that results in higher runoff projections for the future. This doubling of discharge during a low-flow period (a 100% relative increase) although small in absolute terms, can be quite significant from an in-stream flow perspective for fish habitat. Individual GCM responses are not synchronous across basins, which illustrates the importance of selection of GCMs on a regional basis for impact studies.

Emissions scenarios exhibit a range that is smaller than the range in the GCMs and larger than the hydrologic parameterization in these watersheds. Baker Creek exhibits the largest spread in uncertainties across the emissions scenarios. The ranges in runoff anomalies do not follow a distinct pattern in the 2050s; however, by the 2080s, those scenarios with a large projected increase in greenhouse gases (i.e., A2) have larger ranges in runoff anomalies and the range in runoff anomalies per emissions scenarios approximates the GCMs range under the A2 scenario (Table 5). This highlights the need to consider multiple GCMs over multiple emissions scenarios, particularly for planning horizons beyond the mid-twenty-first century.

Hydrological parameterizations and their spread, as illustrated by the range within the boxplots in Fig. 7, indicate variable influences of the selected parameterizations in these watersheds. In general, the hydrologic parameter spread tends to be larger when GCM and emissions anomalies are larger (more positive). This indicates that increasing the amount of runoff in the system leads to greater uncertainty associated with different hydrologic parameterizations. The Ingenika has the greatest range in terms of wintertime spread in variability across the hydrological parameter sets (maximum value of 55%, Table 5, Fig. 7c). Meanwhile, in the summer the Baker Creek watershed has the greatest range in hydrological parameter results, which is largely due to the two B1 scenarios (Table 5, Fig. 7d).

For the two interior subbasins the hydrologic parameterizations are more responsive to the increased projected change in runoff because there is more water in the system to present a wider range of possible outcomes given different soil conditions and precipitation adjustments. The coastal Campbell River system exhibits almost no range in responses to different hydrologic parameterizations during the winter period, as opposed to the other watersheds examined in this study (Table 5). This is likely occurring because of the nature of the Campbell River system (hybrid regime), which has saturated soils throughout the winter; thus the changes to soil parameters have little effect on flow amounts because under almost all circumstances incoming water will exit the basin directly as runoff (see Fig. 4). Therefore, for the Campbell, the hydrologic parameterizations are not as responsive as the effect of different GCMs and emissions scenarios in most seasons. In fall, the maximum range in hydrologic parameterizations is wider than in any other season and closer to the range between emissions scenarios or GCMs.

In the 2080s, the hydrological parameter set spread of runoff uncertainty for the winter is almost always higher than in the 2050s, and in some cases by almost double (Ingenika), although in other watersheds it increases only slightly (Campbell; Table 5). However, GCM and emission scenario uncertainty do not change in equal proportions to the parameter uncertainty in all basins. For example, while the maximum change in hydrological parameters set in Baker Creek increases from 35% to 45% by the 2080s winter, the GCM scenarios range increases from 135% to 258% (Table 5). However, the other two basins appear to follow the pattern of double the 2050s hydrological parameter and GCM emission scenario uncertainty by the 2080s.

The hydrologic parameter, emission, and GCMs uncertainty in summer runoff appears to decrease or stay relatively the same by the 2080s, however, once again the Baker Creek watershed is the exception to this pattern. Baker Creek's summer hydrological parameter uncertainty and GCM uncertainty decrease by approximately half from the 2050s to the 2080s. For this watershed, it is clear that by the 2080s, the B1 temperature projections are high enough to cause a shift in snowpack and/or precipitation is lower. Despite these outliers, in general the hydrological parameter ranges tend to increase particularly in the A1B and A2 scenarios into the 2080s (not shown), suggesting that the scenarios that project greater change out to the longest planning horizons have a stronger influence on response of the model to a range of hydrologic parameterizations (Table 5). This makes sense because as noted above, more robust increases in temperature and precipitation lead to larger shifts in runoff.

Uncertainty in snow water equivalent (SWE) for 1 April SWE was also examined and shows a small but important relative uncertainty response in comparison to runoff (Figs. 7g–i). The available SWE on 1 April is an indication of the amount of snowpack storage that will eventually melt off as runoff, infiltrate into soils, or be held in shallow groundwater reserves over the summer. The range in SWE hydrological parameter sets for Campbell, Ingenika, and Baker is almost negligible, and the range between GCM scenarios for these watersheds is between +20 and −60% in almost all cases (with the exception of one GCM in the Baker Creek watershed). The smaller response in SWE as opposed to runoff is to be expected given that the boxplots (Fig. 7g to 7i) strictly reflect variability because of differences in PADJ and the fact that the range in PADJ values is small (Fig. 4). The Baker Creek and Campbell River watersheds illustrate the same pattern for 2050s SWE—declining snow water equivalent under most scenarios. The Ingenika River basin illustrates slight decreases in SWE according to some GCMs and slight increases according to other models. The 1 April SWE anomalies become increasingly less negative to mixed negative–positive (Campbell versus Ingenika) with increasing basin elevation, which is perhaps an indication that high-elevation snowpacks are being preserved.

The range in summer evapotranspiration (Figs. 7j–l) GCM and emission scenario uncertainty is smaller compared to runoff (approximately ±20%) and reflects both the change in temperature and the amount of water availability (i.e., the PADJ parameter). Available soil water (from precipitation and snowmelt), ET, and soil moisture are linked in terms of their response to climate change (Elsner et al. 2010). In the Ingenika basin, for example, little change or increased SWE along with increased summer rainfall tends to result in modest increases in summer ET because there is available soil moisture stored in the soil column for ET processes (if it has not runoff), which is a known feature of the VIC hydrologic model (Maurer et al. 2010). In the Campbell and the Baker Creek watersheds, where declines in SWE are projected, approximately half of the A1B and A2 scenarios show declines in ET. The range in the ET hydrological parameter set solutions is relatively wide in the Campbell and Ingenika basins in comparison to the lack of variability exhibited in the Baker Creek watershed.

At Baker Creek in winter and summer, and during the summer at the Ingenika basin, most of the median anomalies fall within the range of historical variability for runoff, snow water equivalent, and evapotranspiration (illustrated for runoff, snow water equivalent, and evapotranspiration by the gray boxes in the Figs. 7a–l, and shown in Table 5 as total counts of the GCMs and emissions scenarios that fall outside the range of natural variability, with a maximum value of 15). Although the approach to presenting natural variability could be calculated using more rigorous methods (see Prudhomme and Davies 2009b), the results point to a consideration regarding historic variability in terms of future projected changes. Although changes could appear extreme, it is useful to examine those changes in the context of the historical hydroclimatic regime, particularly in regions of high climatic variability. The projected changes should not be discounted if they fall within the range of natural variability but should be explored further. In the Campbell River system, where all scenarios point to large declines in summer runoff and most 1 April SWE projections are outside the range of natural variability, this can be considered a robust shift in the hydroclimate regime of this watershed.

4. Conclusions

This study assessed uncertainty in the hydrologic responses of watersheds spanning different hydroclimatic regimes for climate change impact analyses. The following sources of uncertainty (i) GCM response, (ii) emissions scenarios, and (iii) hydrologic parameterizations were explicitly analyzed to determine which factor had the greatest amount of uncertainty associated with it for water balance parameters including runoff, snow water equivalent, and evapotranspiration at three unique headwater basins across British Columbia. The major finding is that GCMs, followed by emissions scenarios and then hydrologic parameterizations, exert the greatest influence on uncertainty of impact projections for the water balance parameters analyzed in these three subwatersheds in British Columbia. For the 2050s time period, runoff anomalies examined for winter had the largest range in GCMs over other seasons, emissions scenarios, and the hydrologic parameterizations, in that order, with an average range for all basins of 84%, 58%, and 31%, respectively.

Coastal headwater systems in British Columbia, such as the Campbell River watershed analyzed in this study, may be responding more severely to changes in climate, whereas interior systems (Ingenika) may have storage reserves (i.e., snowpacks at high elevation) that buffer the changes projected by GCMs, resulting in a relatively smaller response. GCMs differences were greatest in a small, headwater system with a responsive hydrologic regime (Baker); in this basin small absolute changes relative to the baseline conditions resulted in large anomaly responses.

The changes observed in this study at the Campbell River watershed fell largely outside of the range of natural variability, a robust shift that may result in a very different future projected for this basin even within the relatively short planning horizon of 50 years. The shifts projected for a small, interior headwater system, Baker Creek, is an example of a system where projected change largely falls within natural variability; however this result necessitates further investigation to consider the full scope of natural variability and how it may be applied in current planning measures. In the Ingenika watershed, all future winter runoff anomalies fall outside of the range of natural variability.

Future work in this area includes expanding the uncertainty analysis to include a greater number of watersheds to sample a wider physiographic range. Further work is required to explore some remaining open questions. These include assessing how the range in uncertainty associated with hydrologic parameterization may be related to watershed size or other physiographic properties. It is also apparent from recent literature (Bae et al. 2011; Maurer et al. 2010) that the choice of hydrologic model can have an impact on uncertainty estimates, such that it would be valuable to assess the effects of model choice on projection uncertainty, particularly in the semiarid watersheds of the province, such as Baker Creek. Understanding the effect of land cover changes (i.e., Mountain Pine Beetle impacts in BC watersheds) is also an important research avenue that could be explored. Improving the assessment of natural variability is a key area of study that could be expanded upon. A complete uncertainty analysis identifying the role of downscaling techniques, hydrologic model selection, emissions scenarios, and GCMs is required for a rigorous assessment of uncertainty in projections of climate change in British Columbian watersheds.

Acknowledgments. The project is funded by BC Hydro and the British Columbia Ministry of Environment and we gratefully acknowledge their support. The BC Hydro Technical Advisory Committee to the Hydrologic Modelling Project (including Allan Chapman, formerly of the British Columbia River Forecast Centre, Brian Menounos of University of Northern BC, Dan Moore of University of BC, and Alex Cannon formerly of Environment Canada) spurred the development of this work. Support from the University of Washington was invaluable in achieving these results; thank you to Alan Hamlet, Marketa Elsner, Ted Bohn, Natalie Voisin, and Dennis Lettenmaier. We thank one anonymous reviewer of this work for his valuable feedback and comments. Anne Berland, formerly of the Pacific Climate Impacts Consortium, is also gratefully acknowledged for assistance with this work.

REFERENCES

Adam, J. C., and D. P. Lettenmaier, 2003: Adjustment of global gridded precipitation for systematic bias. *J. Geophys. Res.,* **108,** 4257, doi:10.1029/2002JD002499.

——, E. A. Clark, and D. P. Lettenmaier, 2006: Correction of global precipitation products for orographic effects. *J. Climate,* **19,** 15–38.

Annan, J., and J. Hargreaves, 2010: Reliability of the CMIP3 ensemble. *Geophys. Res. Lett.,* **37,** L02703, doi:10.1029/2009GL041994.

Arnell, N. W., 1999: Climate change and global water resources. *Global Environ. Change,* **9,** S31–S49.

Bae, D. H., I. W. Jung, and D. P. Lettenmaier, 2011: Hydrologic uncertainties in climate change from IPCC AR4 GCM simulations of the Chungju Basin, Korea. *J. Hydrol.,* **401,** 90–105.

Batjes, N. H., Ed., 1995: A homogenized soil data file for global environmental research: A subset of FAO, ISRIC and NRCS profiles (version 1.0). International Soil Reference and Information Centre Working Paper and Preprint 95/10b, 43 pp.

Bergstrom, S., B. Carlsson, M. Gardelin, G. Lindstrom, A. Pettersson, and M. Rummukainen, 2001: Climate change impacts on runoff in Sweden assessments by global climate models, dynamical downscaling and hydrological modelling. *Climate Res.,* **16,** 101–112.

Bray, D., and H. von Storch, 2009: ''Prediction'' or ''projection''? *Sci. Commun.,* **30,** 534.

Centre for Land and Biological Resources Research, cited 1996: Soil landscapes of Canada, version 2.2. Agriculture and Agri-Food Canada Research Branch. [Available online at http://sis.agr.gc.ca/cansis/nsdb/slc/v2.2/.]

Christensen, N. S., and D. P. Lettenmaier, 2007: A multimodel ensemble approach to assessment of climate change impacts on the hydrology and water resources of the Colorado River Basin. *Hydrol. Earth Syst. Sci.,* **11,** 1417–1434.

Cosby, B. J., G. M. Homberger, R. B. Clapp, and T. R. Ginn, 1984: A statistical exploration of the relationships of soil moisture characteristics to the physical properties of soils. *Water Resour. Res.,* **20,** 682–690.

Daly, C., R. P. Neilson, and D. L. Phillips, 1994: A statistical–topographic model for mapping climatological precipitation over mountainous terrain. *J. Appl. Meteor.,* **33,** 140–158.

——, W. P. Gibson, G. H. Taylor, G. L. Johnson, and P. Pasteris, 2002: A knowledge-based approach to the statistical mapping of climate. *Climate Res.,* **22,** 99–113.

Demarchi, D. A., 1993: Ecoregions of British Columbia. 3rd ed. British Columbia Ministry of Environment, Lands and Parks.

——, cited 1996: An introduction to the ecoregions of British Columbia. Ministry of Environment, Lands and Parks Wildlife Branch. [Available online at http://www.env.gov.bc.ca/ecology/ecoregions/title_author.html.]

Eaton, B., and R. D. Moore, 2010: Regional hydrology. *Compendium of Forest Hydrology and Geomorphology in British Columbia,* R. G. Pike et al., Eds., BC Ministry of Forests and Range, Research Branch, and FORREX Forest Research Extension Partnership, 85–110.

Elsner, M. M., and Coauthors, 2010: Implications of 21st century climate change for the hydrology of Washington State. *Climatic Change,* **102,** 225–260.

FAO, 1995: The digital soil map of the world, version 3.5. Food and Agriculture Organization of the United States (FAO), Rome, Italy, digital media, series 1.

Feddema, J. J., K. W. Oleson, G. B. Bonan, L. O. Mearns, L. E. Buja, G. A. Meehl, and W. M. Washington, 2005: The importance of land-cover change in simulating future climates. *Science,* **310,** 1674–1678.

Fowler, H. J., S. Blenkinsop, and C. Tebaldi, 2007: Review: Linking climate change modelling to impacts studies: Recent advances in downscaling techniques for hydrological modelling. *Int. J. Climatol.,* **27,** 1547–1578.

Gleckler, P. J., K. E. Taylor, and C. Doutriaux, 2008: Performance metrics for climate models. *J. Geophys. Res.,* **113,** D06104, doi:10.1029/2007JD008972.

Global Soil Data Task Group, 2000: Global gridded surfaces of selected soil characteristics (IGBP-DIS). Dataset, doi:10.3334/ORNLDAAC/569. [Available online at http://daac.ornl.gov/cgi-bin/dsviewer.pl?ds_id=569.]

Hamann, A., and T. Wang, 2005: Models of climate normals for genecology and climate change studies in BC. *Agric. For. Meteor.,* **128,** 211–221.

Hamlet, A. F., and D. P. Lettenmaier, 1999: Effects of climate change on hydrology and water resources in the Columbia River Basin. *J. Amer. Water Resour. Assoc.,* **35,** 1597–1623.

——, and ——, 2005: Production of temporally consistent gridded precipitation and temperature fields for the continental United States. *J. Hydrometeor.,* **6,** 330–336.

——, P. W. Mote, M. P. Clark, and D. P. Lettenmaier, 2007: Twentieth-century trends in runoff, evapotranspiration, and soil moisture in the western United States. *J. Climate,* **20,** 1468–1486.

Hayhoe, K., 2010: *A Standardized Framework for Evaluating the Skill of Regional Climate Downscaling Techniques*. University of Illinois, 153 pp.

Horton, P., B. Schaefli, A. Mezghani, B. Hingray, and A. Musy, 2006: Assessment of climate change impacts on alpine discharge regimes with climate model uncertainty. *Hydrol. Processes,* **20,** 2091–2109.

Jarvis, A., and H. I. Reuter, A. Nelson, and E. Guevara, cited 2008: Hole-filled SRTM for the globe, version 4. CGIAR-CSI SRTM 90m Database. [Available online at http://srtm.csi.cgiar.org.]

Kalnay, E., and Coauthors, 1996: The NCEP/NCAR 40-Year Reanalysis Project. *Bull. Amer. Meteor. Soc.,* **77,** 437–471.

Kay, A., H. Davies, V. Bell, and R. Jones, 2009: Comparison of uncertainty sources for climate change impacts: Flood frequency in England. *Climatic Change,* **92,** 41–63.

Knutti, R., 2008: Should we believe model predictions of future climate change? *Philos. Trans. Roy. Soc.,* **366A,** 4647–4664.

——, G. Abramowitz, M. Collins, V. Eyring, P. J. Gleckler, B. Hewiston, and L. Mearns, 2010a: Good practice guidance paper on assessing and combining multi model climate projections. *Meeting Report of the Intergovernmental Panel on Climate Change Expert Meeting on Assessing and Combining Multimodel Climate Projections,* T. F. Stocker et al., Eds., IPCC Working Group I Technical Support Unit, 15 pp.

——, R. Furrer, C. Tebaldi, J. Cermak, and G. A. Meehl, 2010b: Challenges in combining projections from multiple climate models. *J. Climate,* **23,** 2739–2758.

Latifovic, R., cited 2006: Canada 1-km, 10-day SPOT/VEGETATION composites for growing season 1998-2005. [Available online at ftp://ftp.ccrs.nrcan.gc.ca/ad/EMS/LAI/vgtlai/.]

Leavesley, G. H., 1994: Modeling the effects of climate change on water resources —A review. *Climatic Change,* **28,** 159–177.

Liang, X., D. P. Lettenmaier, E. F. Wood, and S. J. Burges, 1994: A simple hydrologically based model of land surface water and energy fluxes for general circulation models. *J. Geophys. Res.,* **99,** 14 415–14 428.

——, E. F. Wood, and D. P. Lettenmaier, 1996: Surface soil moisture parameterization of the VIC-2L model: Evaluation and modification. *Global Planet. Change,* **13,** 195–206.

Lohmann, D., E. Raschke, B. Nijssen, and D. P. Lettenmaier, 1998: Regional scale hydrology: I. Formulation of the VIC-2L model coupled to a routing model. *Hydrol. Sci. J.,* **43,** 131–141.

Ludwig, R., and Coauthors, 2009: The role of hydrological model complexity and uncertainty in climate change impact assessment. *Adv. Geosci.,* **21,** 63–71.

MacKinnon, A., C. DeLong, and D. Meidinger, 1990: A field guide for site identification and interpretation of ecosystems of the Northwest portion of the Prince George Forest Region. Ministry of Forest Land Management Handbook Number 21, 116 pp.

Maurer, E. P., 2007: Uncertainty in hydrologic impacts of climate change in the Sierra Nevada, California, under two emissions scenarioes. *Climatic Change,* **82,** 309–325.

——, A. W. Wood, J. C. Adam, and D. P. Lettenmaier, 2002: A long-term hydrologically based dataset of land surface fluxes and states for the conterminous United States. *J. Climate,* **15,** 3237–3251.

——, L. D. Brekke, and T. Pruitt, 2010: Contrasting lumped and distributed hydrology models for estimating climate change impacts on California watersheds. *J. Amer. Water Resour. Assoc.,* **46,** 1024–1035.

Meehl, G. A., and Coauthors, 2007: The WCRP CMIP3 multimodel dataset: A new era in climate change research. *Bull. Amer. Meteor. Soc.,* **88,** 1383–1394.

Minville, M., F. Brissette, and R. Leconte, 2008: Uncertainty of the impact of climate change on the hydrology of a nordic watershed. *J. Hydrol.,* **358,** 70–83.

Moore, R., J. Trubilowicz, and J. Buttle, 2011: Prediction of streamflow regime and annual runoff for ungauged basins using a distributed monthly water balance model. *J. Amer. Water Resour. Assoc.,* **48,** 32–42.

Murphy, J., B. Booth, M. Collins, G. Harris, D. Sexton, and M. Webb, 2007: A methodology for probabilistic predictions of regional climate change from perturbed physics ensembles. *Philos. Trans. Roy. Soc.,* **365A,** 1993–2028.

Nakicenovic, N., and Coauthors, 2000: *Special Report on Emissions Scenarios*. Intergovernmental Panel on Climate Change, 27 pp.

Nash, J. E., and J. V. Sutcliffe, 1970: River flow forecasting through conceptual models part I—A discussion of principles. *J. Hydrol.,* **10,** 282–290.

Nawaz, N., and A. Adeloye, 2006: Monte Carlo assessment of sampling uncertainty of climate change impacts on water resources yield in Yorkshire, England. *Climatic Change,* **78,** 257–292.

Prudhomme, C., and H. Davies, 2009a: Assessing uncertainties in climate change impact analyses on the river flow regimes in the UK. Part 2: Future climate. *Climatic Change,* **93,** 197–222.

——, and ——, 2009b: Assessing uncertainties in climate change impact analyses on the river flow regimes in the UK. Part 1: Baseline climate. *Climatic Change,* **93,** 177–195.

——, D. Jakob, and C. Svensson, 2003: Uncertainty and climate change impact on the flood regime of small UK catchments. *J. Hydrol.,* **277,** 1–23.

Quick, M. C., 1995: The UBC watershed model. *Computer Models of Watershed Hydrology,* V.P. Singh, Ed., Water Resources Publications, 1144 pp.

Radic, V., and G. K. C. Clarke, 2011: Evaluation of IPCC models performance in simulating late twentieth-century climatologies and weather patterns over North America. *J. Climate,* **24,** 5257–5274.

Randall, D. A., and Coauthors, 2007: Climate models and their evaluation. *Climate Change 2007: The Physical Science Basis,* S. Solomon et al., Eds., Cambridge University Press, 589–662.

Rawls, W. J., L. R. Ahuja, D. L. Brakensiek, and A. Shirmohammadi, 1993: Infiltration and soil water movement. *Handbook of Hydrology,* D. R. Maidment, Ed., McGraw-Hill.

Salathe E. P., Jr., 2005: Downscaling simulations of future global climate with application to hydrologic modeling. *Int. J. Climatol.,* **25,** 419–436.

——, P. W. Mote, and M. W. Wiley, 2007: Review of scenario selection and downscaling methods for the assessment of climate change impacts on hydrology in the United States Pacific Northwest. *Int. J. Climatol.,* **27,** 1611–1621.

Schnorbus, M., K. E. Bennett, and A. T. Werner, 2010: Quantifying the water resources impacts of Mountain Pine Beetle and associated salvage harvest operations across a range of watershed scales: Hydrologic modelling of the Fraser River basin. Canadian Forest Service Information Rep. BC-X-423, 64 pp.

Shepard, D. S., 1984: Computer mapping: The SYMAP interpolation algorithm. *Spatial Statistics and Models,* G. L. Gaile and C. J. Willmott, Eds., D. Reidel, 133–145.

Shi, X., A. W. Wood, and D. P. Lettenmaier, 2008: How essential is hydrologic model calibration to seasonal streaflow forecasting? *J. Hydrometeor.,* **9,** 1350–1363.

Singh, V. P., and D. A. Woolhiser, 2002: Mathematical modeling of watershed hydrology. *J. Hydrol. Eng.,* **7,** 270.

Stahl, K., R. D. Moore, J. A. Floyer, M. G. Asplin, and I. G. McKendry, 2006a: Comparison of approaches for spatial interpolation of daily air temperature in a large region with complex topography and highly variable station density. *Agric. For. Meteor.,* **139,** 224–236.

——, ——, and I. G. McKendry, 2006b: The role of synoptic-scale circulation in the linkage between large-scale ocean-atmosphere indices and winter surface climate in British Columbia, Canada. *Int. J. Climatol.,* **26,** 541–560.

Tebaldi, C., R. L. Smith, D. Nychka, and L. O. Mearns, 2005: Quantifying uncertainty in projections of regional climate change: A Bayesian approach to the analysis of multimodel ensembles. *J. Climate,* **18,** 1524–1540.

Todd, M., R. Taylor, T. Osborn, D. Kingston, N. Arnell, and S. Gosling, 2011: Uncertainty in climate change impacts on basin-scale freshwater resources–preface to the special issue: The QUEST-GSI methodology and synthesis of results. *Hydrol. Earth Syst. Sci.,* **15,** 1035–1046.

Wang, T. L., A. Hamann, D. L. Spittlehouse, and S. N. Aitken, 2006: Development of scale-free climate data for western Canada for use in resource management. *Int. J. Climatol.,* **26,** 383–397.

Werner, A., 2011: BCSD downscaled transient climate projections for eight select GCMs over British Columbia, Canada. University of Victoria Pacific Climate Impacts Consortium Rep., 63 pp.

Widmann, M., C. S. Bretherton, and E. P. Salathe Jr., 2003: Statistical precipitation cownscaling over the northwestern United States using numerically simulated precipitation as a predictor. *J. Climate,* **16,** 799–816.

Wood, A. W., E. P. Maurer, A. Kumar, and D. P. Lettenmaier, 2002: Long range experimental hydrologic forecasting for the eastern U.S. *J. Geophys. Res.,* **107,** 4429, doi:10.1029/2001JD000659 .

——, L. R. Leung, W. Sridhar, and D. P. Lettenmaier, 2004: Hydrologic implications of dynamical and statistical approaches to downscaling climate model outputs. *Climatic Change,* **62,** 189–216.

Wulder, M., M. Cranny, and J. Dechka, 2002: An illustrated methodology for land cover mapping of Forests with Landsat-7 ETM+ data: Methods in support of EOSD land cover, version 2. Natural Resources Canada, Canadian Forest Service, Pacific Forestry Centre Rep., 39 pp. [Availablel online at http://www.pfc.forestry.ca/ eosd/cover/Methods_vers2_e.pdf.]

Yapo, P. O., H. V. Gupta, and S. Sorooshian, 1998: Multi-objective global optimization for hydrologic models. *J. Hydrol.,* **204,** 83–97.